



**University of
Sunderland**

Hassani, Vahid, Khabazi, Zubin, Ahmad Mehrabi, Hamid, Gregg, Carl and O'Brien, Roger (2020) Rationalization Algorithm for a Topologically-Optimized Multi-Branch Node for Manufacturing by Metal Printing. *Building Engineering*, 29. ISSN 2352-7102

Downloaded from: <http://sure.sunderland.ac.uk/id/eprint/11416/>

Usage guidelines

Please refer to the usage guidelines at <http://sure.sunderland.ac.uk/policies.html> or alternatively contact sure@sunderland.ac.uk.

Rationalization Algorithm for a Topologically-Optimized Multi-Branch Node for Manufacturing by Metal Printing

Vahid Hassani¹, Zubin Khabazi², Hamid Ahmad Mehrabi³, Carl Gregg⁴, Roger William O'Brien⁵

¹Sustainable Advanced Manufacturing (SAM), University of Sunderland,
vahid.hassani@sunderland.ac.uk

²Singapore University of Technology and Design,
zubin@morphogenesisism.com

³Sustainable Advanced Manufacturing (SAM), University of Sunderland,
hamid.mehrabi@sunderland.ac.uk

⁴Sustainable Advanced Manufacturing (SAM), University of Sunderland,
carl.gregg@sunderland.ac.uk

⁵Sustainable Advanced Manufacturing (SAM), University of Sunderland,
Roger.O'Brien@sunderland.ac.uk

¹Vahid Hassani, <https://orcid.org/0000-0001-6724-2520>

²Zubin Khabazi, <https://orcid.org/0000-0002-8956-9679>

³Hamid Ahmad Mehrabi, <https://orcid.org/0000-0003-0510-4055>

⁴Carl Gregg, <https://orcid.org/0000-0002-6033-4104>

⁵Roger William O'Brien, <https://orcid.org/0000-0001-6898-0875>

ABSTRACT

In the last few years, additive manufacturing (AM) technologies has enabled engineers to design and develop several products with complex geometries, which could not be easily built by conventional manufacturing methods. Furthermore, AM application has been extended from solely making prototypes to develop end-use components in different industry sectors such as civic, aerospace, medical and etc. One of the earliest additive manufacturing methods known as metal printing allows us to produce more performative components in industries, however due to some limitations, this method claims different strategies of design for additive manufacturing (DFAM). In this research, a construction component, namely multi branch node, which is used in space frame (SF), is chosen as a platform in order to implement the design strategy on its surface using a rationalization algorithm. At first, a multi branch node is simply sketched using the dimensional information of SF's converging bars into a specific node. Then, a topology optimization analysis is performed by reducing the aforementioned volume from the specific section of the node to achieve the minimum strain energy. Finally, a rationalization algorithm namely, mesh-matching technique is implemented on a topologically-optimized node in order to make it more compatible with the metal printing and additionally provide safety and structural advantages compared to the original node.

Keywords: Additive Manufacturing Technologies; Design for Additive Manufacturing; Rationalization Algorithm; Mesh-Matching Technique; Topology Optimization; Metal 3D-Printing;

1. Introduction

As the configuration of industrial components tends toward increasing complexity, thanks to the recent development of AM technologies that offer unique capabilities and design freedoms, the form-finding and rationalization strategies have gained much of interests among the research teams due to this development. In civic sector, these strategies need to be defined to ensure the efficient use of material, easy buildability, structural reliability and safety functionality of the entire system.

The emergence of AM technologies on the one hand, has given a roadmap to researchers and engineers to redesign the components with higher manufacturing freedoms. And on the other hand, the progress in digital design and development of a numerical methods enables manipulation of constitutive elements of a given geometry to increase its complexity both formally and configurationally [1,2].

As a consequence of progress in both digital design and AM technologies, the term, rationalization, is highlighted because of its importance in buildability of engineering products. Rationalization is a work-flow that maps from design-to-build process and attempts to create a systematic methodology to translate from conceptual design to end-use product while the technical problems are addressed during the translation [3]. More specifically, rationalization strategy, which is widely used in contemporary architectural projects, is a strategy to use maximum capabilities of digital fabrication processes and CAD environment to translate the theoretical design of the objects with complex geometries into practice according to the constraints of fabrication [4]. In other words, this method is used to reconfigure and transform the complex forms from the CAD environment into physical reality. The most important advantages of this strategy is the scale that includes the wide range of small-scale components to even large-scale buildings. Recently, considerable attention has been paid to this method in architecture. E.g., Schlueter and Bonwetsch [5] worked on a design project called “ANAN”, a Japanese noodle bar, in which a digital design toolbar was utilized to facilitate the rationalization and production of the elements in a cellular design manner. Rationalization, in other viewpoint, can be considered as common intersection point between several disciplines such as social sciences, mathematics, engineering and architecture [6]. One of the useful tools for connection between most of the mentioned disciplines and realizing the interaction between them is the parametric design. Currently, parametric design enables architectures to implement the rationalization strategies in digital environment more appropriately, however the interplay between the architectural and structural aspects needs to be further explored [7]. An innovative geometry rationalization method is introduced for some non-standard architectural buildings and the impact on the future relationship and integration between architectural and structural engineering is investigated [8].

The focus of recent research has been on implementing the rationalization and form-finding methods to address the issues created due to fabrication and manufacturing constraints. In architectural engineering, to meet the constraints mentioned above, two frameworks are commonly used to model the irregular and regular curved surfaces namely, non-uniform rational basis spline (NURBS) and mesh-based approach, which create somewhat mathematical complexity and high computational time. As an alternative to two frameworks, Mensil et al. [9], proposed generalized cyclidic nets that employs base circular mesh and Dupin cyclides, known as Mobius geometry. This method is recommended as a useful method for shape modeling of circular curved shapes, however for modeling of irregular closed surfaces has not been examined yet. Easy buildability

and fabrication of products that are designed by freeform surface modeling have been always one of the main goals of researchers in this line of research. For this purpose, a design rationalization method is proposed by Darvishani-Fikouhi [10] by which the algorithm is seeded using combination of dynamic relaxation and particle spring methods. In this context, Zaremba [11] used genetic algorithm for fitting buildable arcs into initial curves of a freeform roof structure which was designed by NURBS. The construction process of a freeform architecture was studied in an integrated manner with executable general CAD/CAM design [12]. In another research, the buildability of complex architectural elements was evaluated corresponding to the fabrication machinery which was used to produce them [13]. The developed tool in this research enables researchers to adopt the mesh-based design with the fabrication process. For another type of structure, a novel discretization of freeform surfaces was performed based on four, five, six or seven sided planar elements [14]. The connecting elements are made of steel bars and filled with planar glass plates. Alternatively, planar quadrilateral (PQ) meshes can be used to design and develop nearly smooth freeform surfaces by single-curved panels to avoid exploitation of double-curvature glass, which is not easily buildable [15].

Previous studies indicate that by using digital tools, the freeform surfaces can be rationalized and form-found to be fabricated more easily [16]. In this regard, the digital tools were investigated in terms of form generation, structural analysis and also integration of fabrication and construction process [17].

To date, to the author's knowledge, the rationalization of topologically-optimized SF's nodes with irregular and complex geometry has been scarcely investigated from the aspect of possibility of using metal AM in building industry. Topology optimization of SF's node has been discussed, but these articles have not studied the rationalization process of such products [18,19]. On the completion of previous researches, this research aims to propose a rationalization algorithm for the SF's nodes that possesses irregular shapes with complex geometry. This method relies on the particular capabilities of CAD software to sketch the simple original part, topology optimization of the original geometry and finally rationalization and form-finding of the topologically-optimized node by using mesh matching technique between the desired node geometry and the topologically-optimized node. In comparison with the former proposed rationalization methods, this method is acclaimed due to its flexibility in choosing the intensity of rationalization for any types of closed surfaces with irregular geometry, simplicity of the method and scalability. Ease of manufacturing of the final parts is also considered in metal AM framework and the comparison between the original topologically-optimized node and the rationalized ones is made.

The remainder of the paper is organized as follows. In Section 2, AM capabilities offered in topology optimization and rationalization are discussed. In Section 3, the rationalization process will be discussed in detail. Section 4 compares some nodes with different degrees of rationalization in terms of some advantages offered by the method. Some conclusions will be wrapped up in Section 5.

2. Additive Manufacturing, Topology Optimization and Rationalization

AM is well-known as a process through which an object is built by material addition in layer-by-layer manner. This capability enables for fabrication of the parts and tools of high complexity [20, 21]. In recent years, AM's metal methods, in particular selective laser melting (SLM), selective

laser sintering (SLS) and binder jetting (BJ) have offered a feasible manufacturing solution for manufacturing of components of different industry sectors with complex geometry and higher functionality. Of the three metal AM mentioned above, in SLS and SLM, laser selectively melts particles of metal powder recoated on the build platform with a specific thickness until the components are fabricated with different sorts of complexity and relative density close to 100% [21]. Alternatively, BJ is a process in which a liquid binding agent is selectively deposited through inkjet print nozzles to join powder materials in a powder bed [22]. In this method, the dispensed material is not the build material, but it is used to bond layers of powder in the desired shape. This process is followed by de-binding and sintering processes through which the part gains final strength. In contrast to SLS and SLM methods, BJ creates parts/components with lower strength, but no support structure is generated in this method unlike SLS and SLM methods, meanwhile shorter time is spent for post-processing. For this reason, in order to reduce the support structure generated, new rules and strategies are necessary for DFAM, especially when the complexity of the parts is increasing.

One of the sources of complexities in the design of components is to use topology optimization method [23]. Topology optimization is a tool by which the optimal material distribution is calculated in a given specific mass/volume. Conventional manufacturing methods mostly failed to accomplish building topologically-optimized parts. Recently, due to rapid development of AM technologies, the tendency of designers to build topologically-optimized parts has been increasing [24, 25]. Since AM methods, particularly metal AM, are yet under development, they also have specific issues which need to be well-addressed in order to determine an appropriate DFAM. Concerns such as support structure will restrict the freedoms for engineers to realize their designs in reality. In addition, CAD and engineering software which are used for topology optimization, generate configurations with rough meshes as shown in Figure 1a. Nevertheless, they mostly have rendering option to smooth the rough meshes to smoothed one as shown in Figure 1b, however the rendering capability cannot completely ensure some design aspects in terms of the buildability/printability, safety and structural performance of the topologically-optimized parts.



Figure 1. a) Original Topology Optimized Node, b) Node with Smoothed Mesh by Software, [21]

As discussed earlier, rationalization is one of the tools that enable engineers to realize their designs and fulfill the buildability of their products. In this study, to meet the design objectives using purposeful rationalization method, a mesh-matching technique is proposed. This method is solely used for the rationalization of a multi-branch SF's node which connects the converging bars in a space frame structure generated by vMESH system [26] and illustrated in Figure 2. This technique relies on the matching between the mesh structure of the desired configuration of the node that is generated by Exoskeleton plug-in [27, 28] and the mesh structure of the topologically-optimized node in Grasshopper environment. This technique allows us to tune the distance between the neighboring meshes of two structures in order to have the different smoothing degree at final node. Implementing this technique, the following goals can be achieved:

- 1) The new technique will create the smooth edges on the central part of the node that are originally sharp due to topology optimization. The initial sharp edges are not safe to work with.
- 2) Smooth edges will generate less stress concentration compared to the initial sharp edges.
- 3) In terms of AM requirements, the smooth edges are much easier for 3D printing especially when SLM and SLS are used and the support structure is generated consequently.

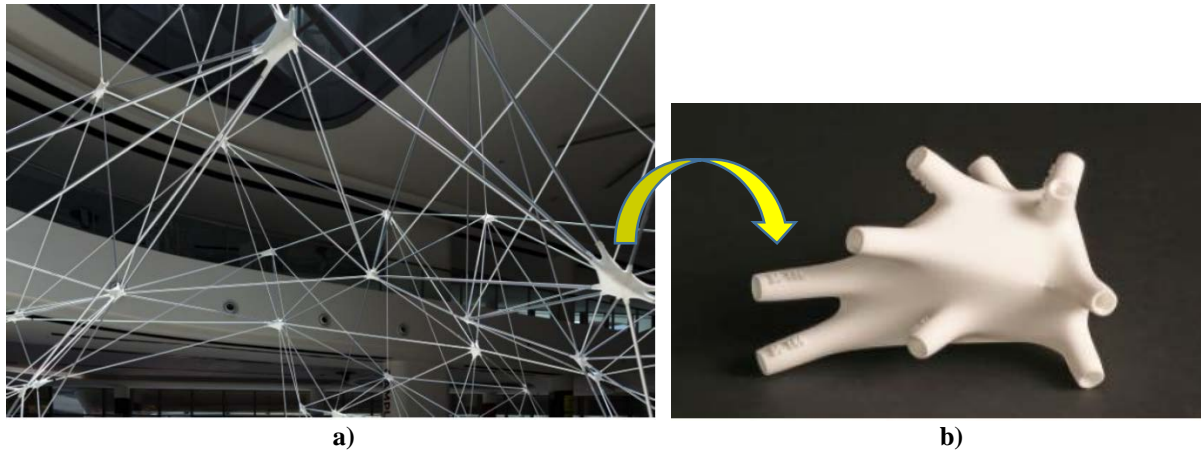


Figure 2. a) Randomly Generated vMESH Structure, b) Connecting SF Node, [27]

3. Node Sketching, Topology Optimization and Rationalization

This section describes the rationalization procedure of the SF's node in three steps namely, node sketching, topology optimization and design rationalization that can be applied to all types of spherical nodes as shown in Figure 3. The method, discussed in this section, is implemented at different CAD environments in order to take advantage of their unique capabilities. SolidWorks for sketching and topology optimization, ExoWireframe as one of the components in Grasshopper for node geometric modeling, mesh-matching and design rationalization and finally Rhinoceros software for rendering and realization of the model generated by Grasshopper. The digital workflow is shown schematically in Figure 4.



Figure 3. Examples of Space Frame Spherical Node

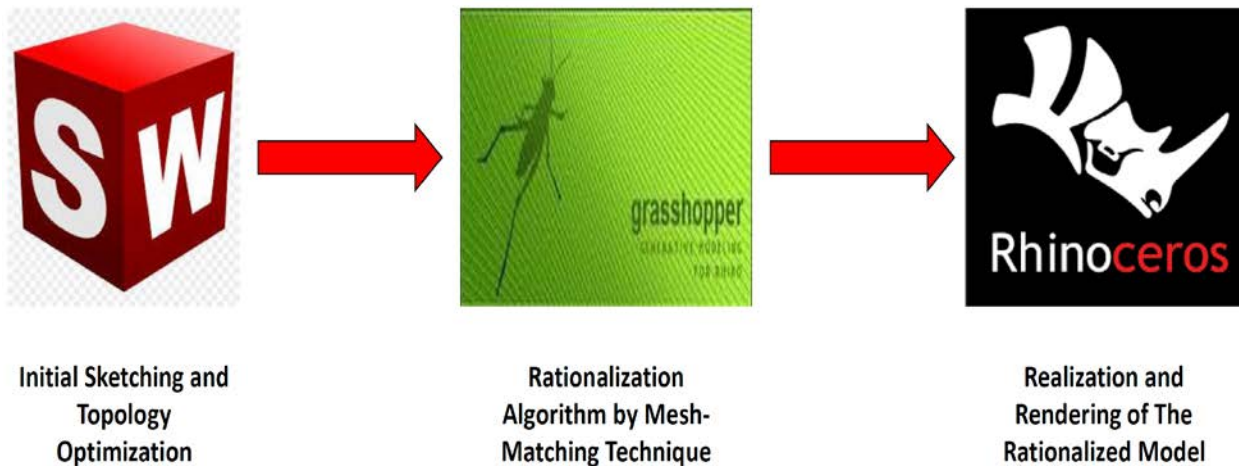


Figure 4. Overview of Rationalization Process

3.1. Node Sketching

As discussed earlier, the node is sketched based on the information of a pre-designed SF structure like shown in Figure 2a. Using the dimensional information of the blank space where the SF bars are converged, the length of the node's branches and their orientation will be determined. Initially, the node is sketched in the SolidWorks environment. SolidWorks enables us to sketch a combination of points, lines and solid parts in a sequential manner.

In order to start sketching of the node, firstly the intersection point is set to (0,0,0) in 3d-space and all branches are connected to this point as shown in Figure 5.

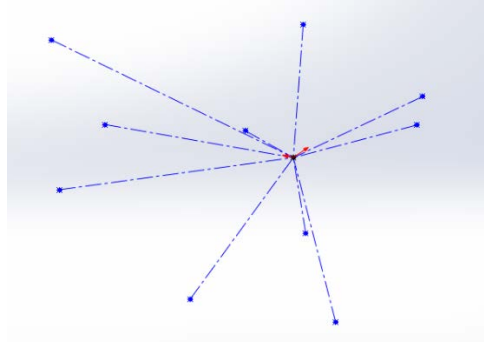


Figure 5. Initial Drawing of Intersection Point at SolidWorks Software

To create the initial node geometry, a sphere is sketched centered at the intersection point of the node. The radius of the sphere is chosen as the length of the smallest branch subtracted by 15mm i.e. 23.8mm for this case as shown in Figure 6. Note should be taken that these branches are connected to converging bars either by welding or screwing. In case, when the converging bars are screwed to the branches, the depth of screw inside the bar is chosen 10mm and 5mm for the intermediate solid section between screw and the surface of sphere. The depth of screw is shown in Figure 7 to visualize how the radius of sphere is selected for a specific node.

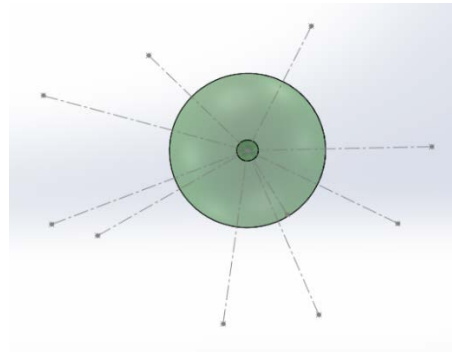


Figure 6. Central Sphere Centered at the Intersection Point, $R = 23.8\text{mm}$

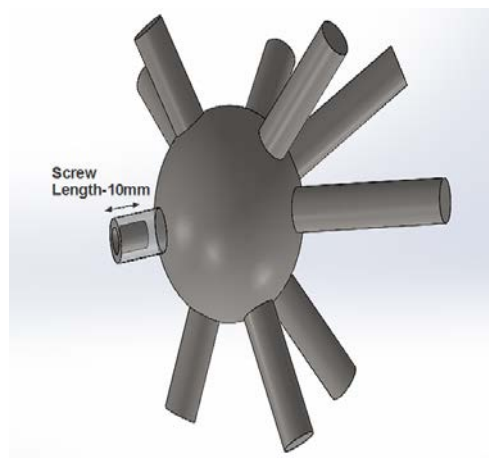


Figure 7. The Depth of Screw inside the Smallest Branch

After creating the central sphere, all cylindrical branches are sketched and attached to the surface of sphere. Then, a plane perpendicular to the connecting lines of each branch to the intersection point, is created. On each plane, a circle with diameter of 10mm is sketched and the sketch is extruded up to the surface of sphere and the entire node is completed (see figures 8 and 9).

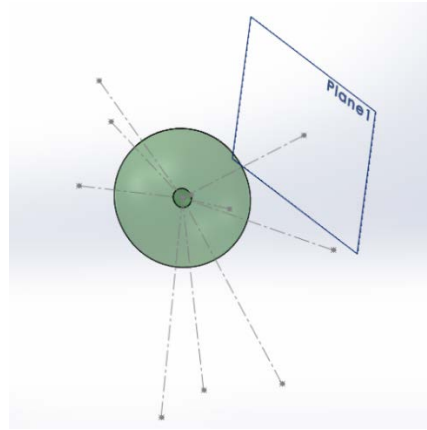


Figure 8. Perpendicular Plane to each Branch to Create the Cylindrical Branch

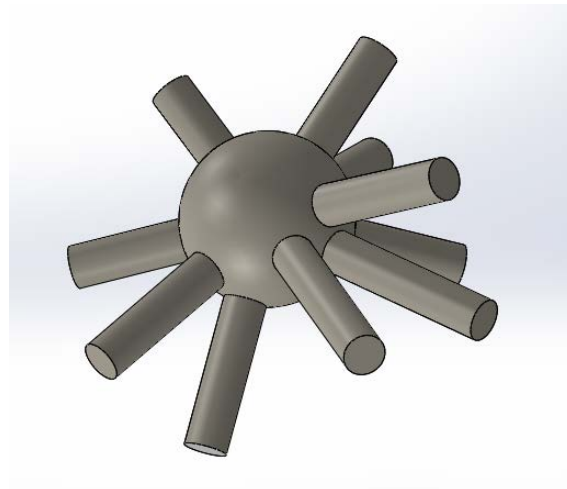


Figure 9. Solid Form of the Spherical Node

3.2. Topology Optimization

After sketching the spherical node in SolidWorks software, the topology optimization is performed based on the minimization of the strain energy (maximization of stiffness). In this analysis, the optimal mass distribution is calculated based on the given volume/mass reduction in SolidWorks environment. The magnitude of loads applied to each branch along their normal direction is shown in Figure 10. These loads were calculated using a separate analysis on SF structure using KARAMBA software [29]. The material was chosen to be 17-4 PH stainless steel used in Markforged metal printers. The mechanical properties for the material is given in Table 1 after sintering process.

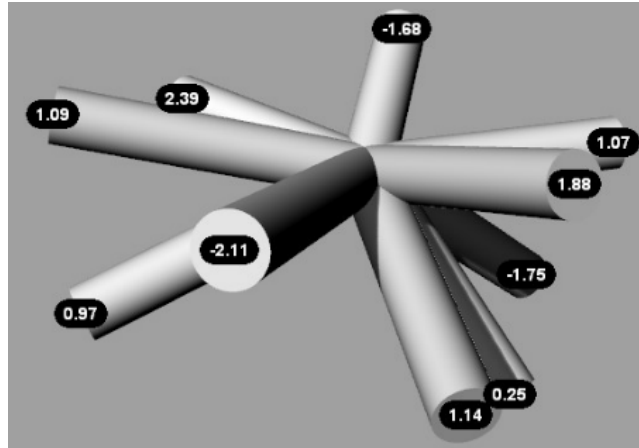


Figure 10. Load applied on each Branch's Surface (KN)

To define the boundary conditions of the model for this analysis, the face of all branches connected to the converging bars are assumed to be fixed with zero displacement along local tangential t_1 and t_2 directions and free to move along the normal, n direction of each branch. Figure 11 shows the local coordinate of one branch's surface including three orthogonal elements namely, t_1 , t_2 and n (local normal direction).

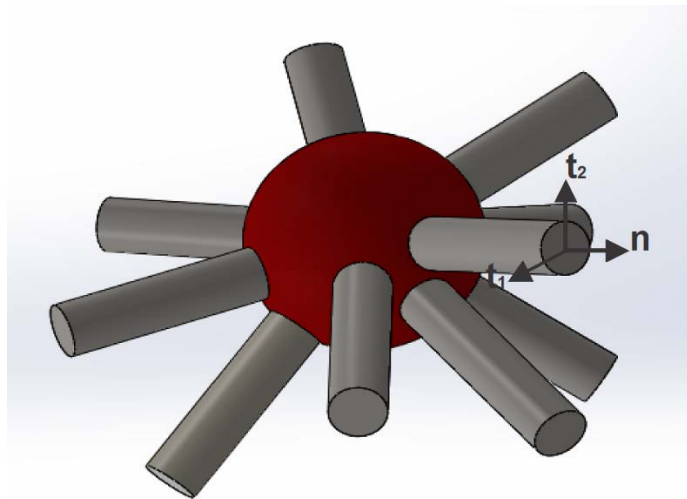


Figure 11. Local Coordinates at Branch's Surface

In order to match the mesh structures between the desired node generated by Exoskeleton plug-in in Grasshopper software and the topologically-optimized node generated by topology optimization toolbox of SolidWorks software, which will be discussed in Section 3.3, no discontinuity in the topologically-optimized node is allowed. This refers to as the limitation of Exoskeleton plug-in. Furthermore, Discontinuities in the structure of central sphere will necessitate the generation of support structure through metal printing process and the removal of support structure will be difficult or sometime impossible for such irregular geometries. The percentage of mass reduction is chosen such that no discontinuity occurs in the solid form of the topologically-optimized node. The percentage of mass reduction varies depending on the configuration, material of the node and the applied load. Analysis in this research shows an optimum value of 30% mass reduction from

the original mass. However, increasing mass reduction from 30% up to 35% is accompanied with discontinuity in the structure as shown in Figure 12. This is achieved in a trial and error manner within the topology optimization process and has to be considered to support the proper manufacturing of the node by metal printing.

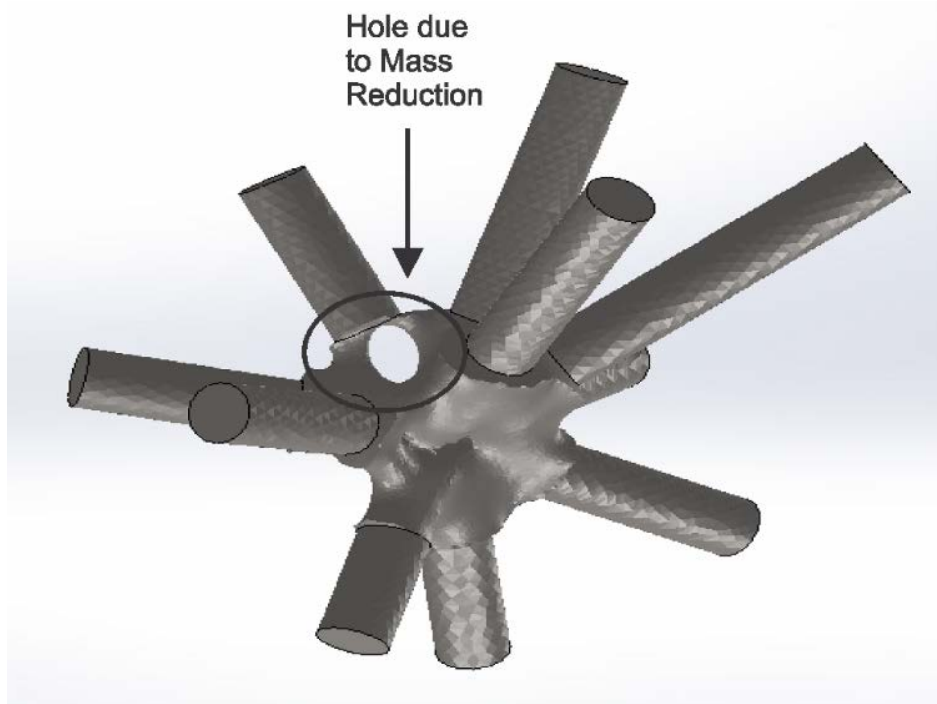
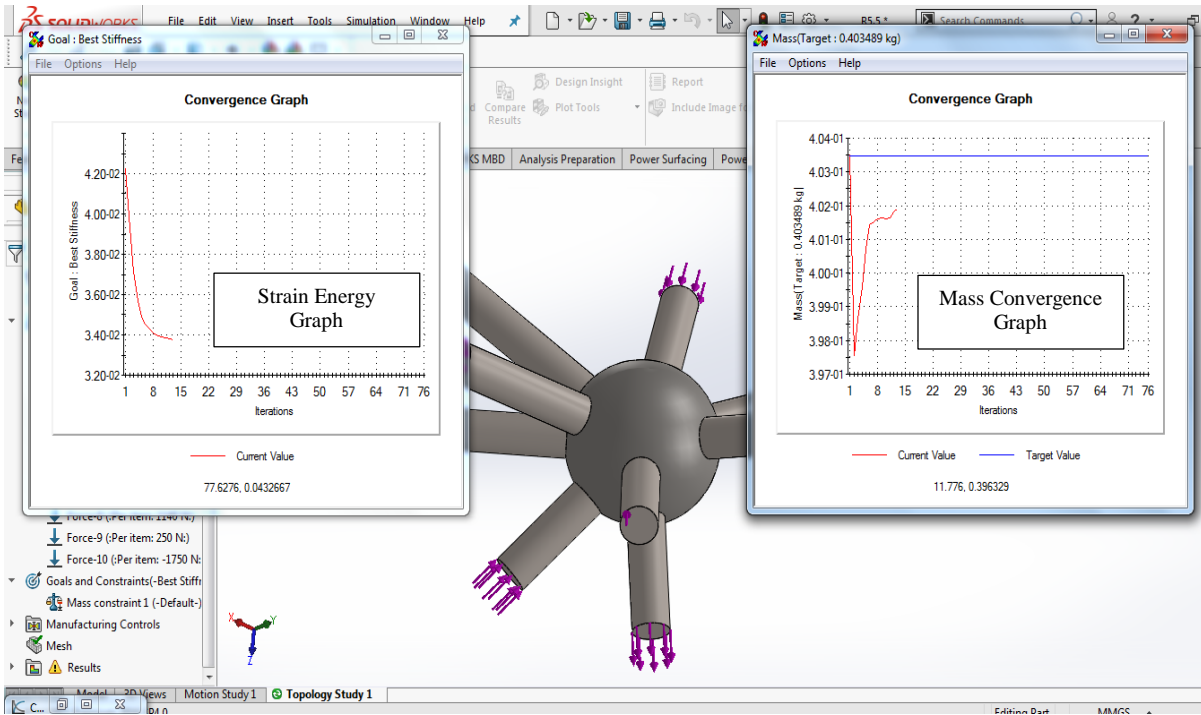


Figure 12. Created Discontinuity at Node due to Excessive Mass Reduction during the Topology Optimization Process

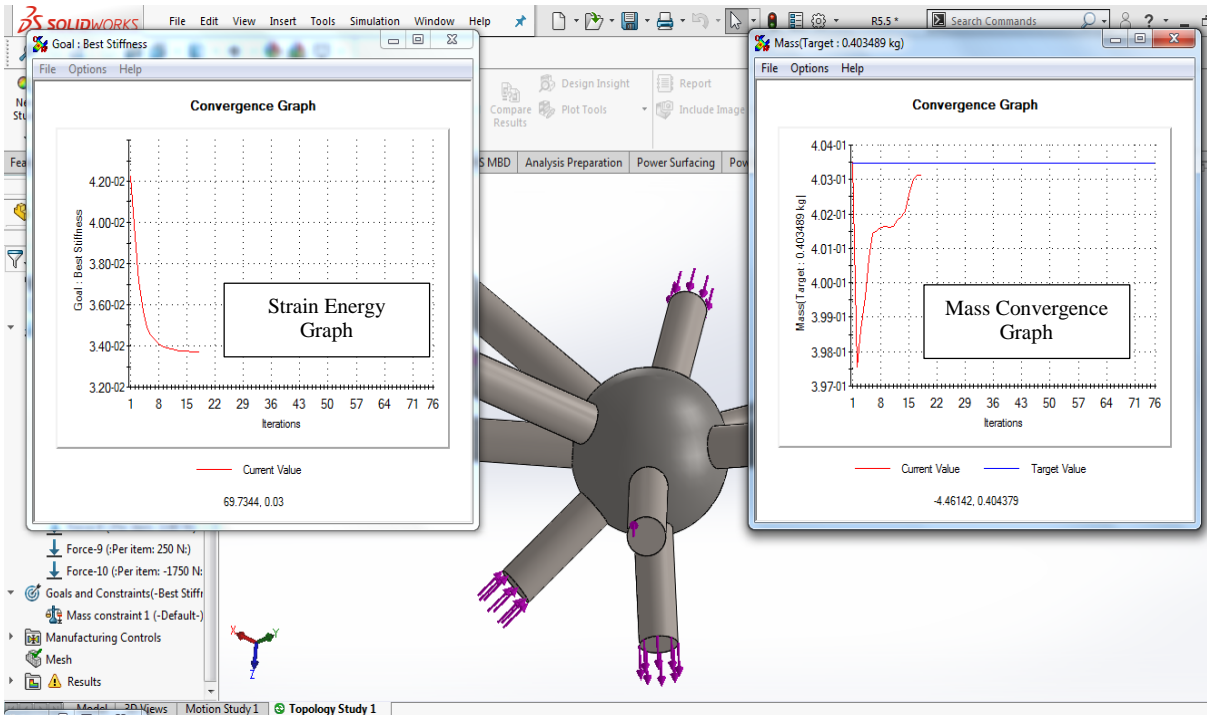
Figure 13 shows the topology optimization process carried out based on the minimization of strain energy minimization (stiffness maximization) and the convergence of the node mass to target mass of 0.4 kg in this case. The final result of topologically-optimized node is shown in Figure 14 that consists of irregular geometry with sharp edges. This configuration might not be promising in terms of printability by metal printers, safety functionality, appearance and structural performance.

Table 1. Mechanical Properties of 17-4 PH stainless steel

Mechanical Properties	Quantity
Young's Modulus	170 GPa
Yield Strength	1100 MPa
Tensile Strength	1250 MPa
Poisson's Ratio	0.3
Density	7860 kg/m³



a)



b)

Figure 13. Topology Optimization Procedure: a) Initial Stage of Optimization b) Final Stage of Optimization

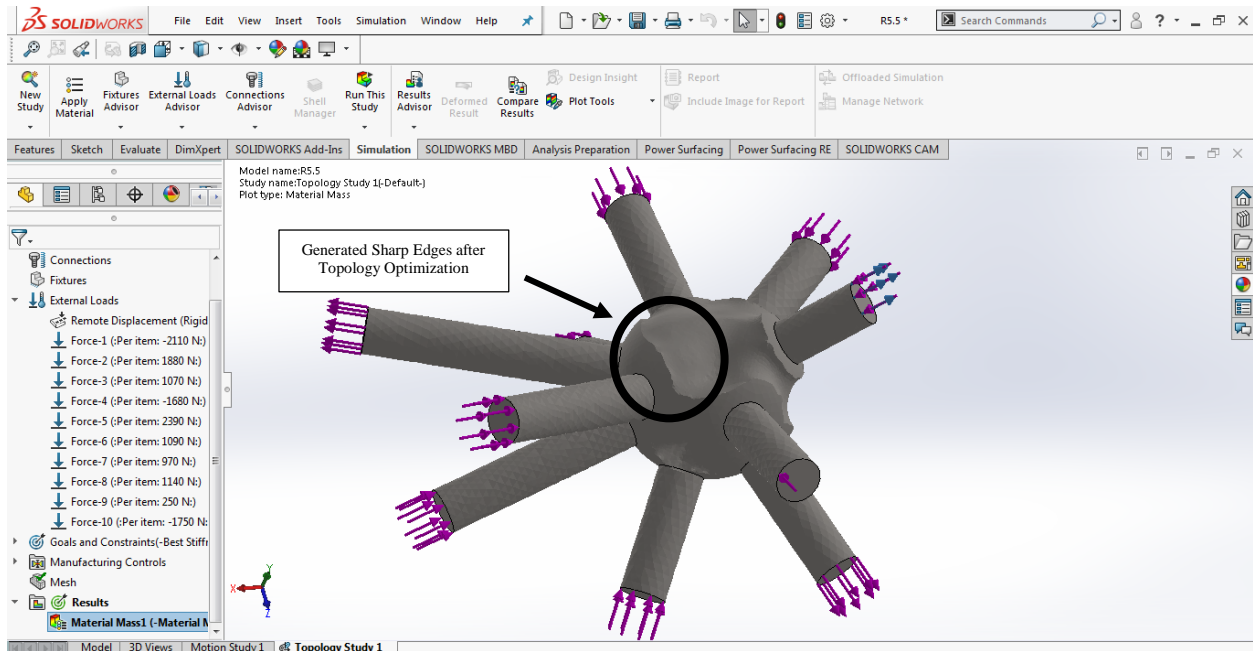


Figure 14. Final Configuration of the Node after Topology Optimization

3.3. Design Rationalization of the Topologically-Optimized Node for Metal Printing

The output of the topology optimization is basically a rough mesh with lots of local sharp edges and indents and even not a global desirable object for manufacturing. There are various algorithms, which can be used to smooth this mesh, but it is not always ensured to remove all such little indentations and produce a continuous smoothed surface. On the other hand, as discussed, the ExoWireframe component can create a multi-branch node with a continuous surface, which is geometrically smooth but not optimized structurally, and perhaps results in a larger volume/mass. In order to produce a node with both desired geometry and volume, the problem should be addressed.

The ExoWireframe creates a solid mesh across a network of connected lines. This mesh is the thickened joint of all those lines as volumetric elements (cylinders), wrapped together with a one single smooth geometry. It is possible to define the radius of the cylinders as well as a global parameter to control the size (volume) of the node. Yet with this global parameter, it is not straightforward to control the local properties of the node, like local removal of material from its volume. Having hundreds of such nodes in a structure means using extra material, causing increase in material consumption and cost, printing time and finally extra weight to the structure. Here the main idea is to develop an algorithm which adapts the topologically-optimized mesh to the ExoWireframe one, so not only it would be geometrically fine, but also optimized in its volume/mass.

The rationalization algorithm uses the best part of these meshes. In the process, the ExoWireframe mesh (EXO-mesh) is generated (with numerical values set in such a way) to be large enough to contain the topologically-optimized mesh (TO-mesh) inside it. We superimpose it to the TO-mesh as shown in Figure 15, sharing the center point at (0,0,0). The next step is to create a matrix of vectors $[V]$ in which $v(i)$ is the vector from vertex (i) of the TO-mesh to its closest point on the

EXO-mesh. Another matrix [L] is also created in which $l(i)$ is the distance of the vector (i) shown in figures 16a and 16b, $l(i)=|v(i)|$, where [L] denotes the deviation distances of both meshes. The rationalization algorithm attempts to adjust these distances to a predefined value. Therefore, a translation matrix [T] is set up where $t(i)=a * l(i)$ in which “a” is real number between 0 and 1. This modifies the TO-mesh, translating its vertices with values of [T], towards the EXO-mesh (using the same vector directions [V], see Figure 17). Setting “a” to 0 will result in zero displacement which geometrically means no modification and keeping the original TO-mesh, while setting “a” to 1 means the maximum displacement and almost reaching the EXO-mesh. So we are seeking an “a” value by which it creates a smooth mesh, yet with locally-manipulated surface to reach the minimum excessive material as illustrated in figures 18 and 19. The geometry of the node, the volume difference and the weight of excessive material can be monitored in a live feedback mode, both in the viewport and in tables, so to decide how much extra weight the node might need in order to reach to a finer geometrical output. Thus the adaptation percentage can be changed, either push the mesh further towards a finer surface or remain closer to the original optimized one (Figure 19).

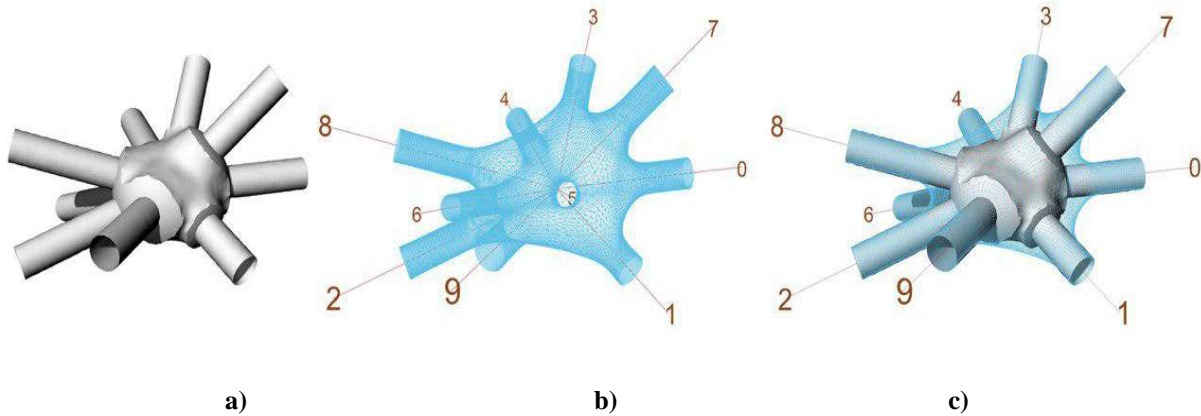


Figure 15. a) TO-Mesh, b) EXO-Mesh and c) Superimposition of both Meshes

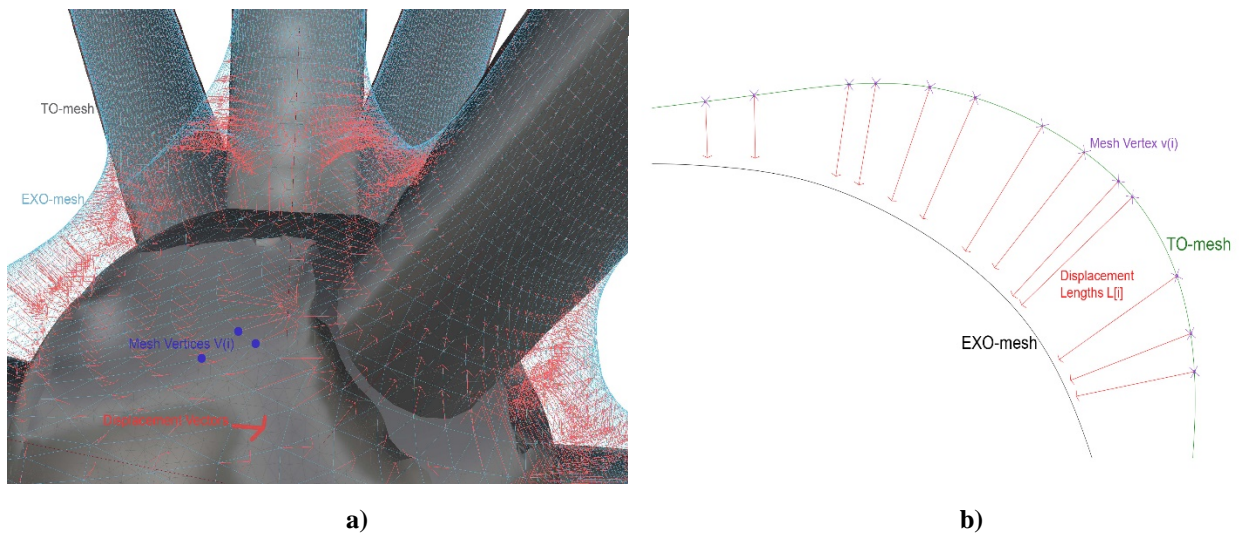


Figure 16. Distance $l(i)$ between Exo-Mesh and TO-Mesh

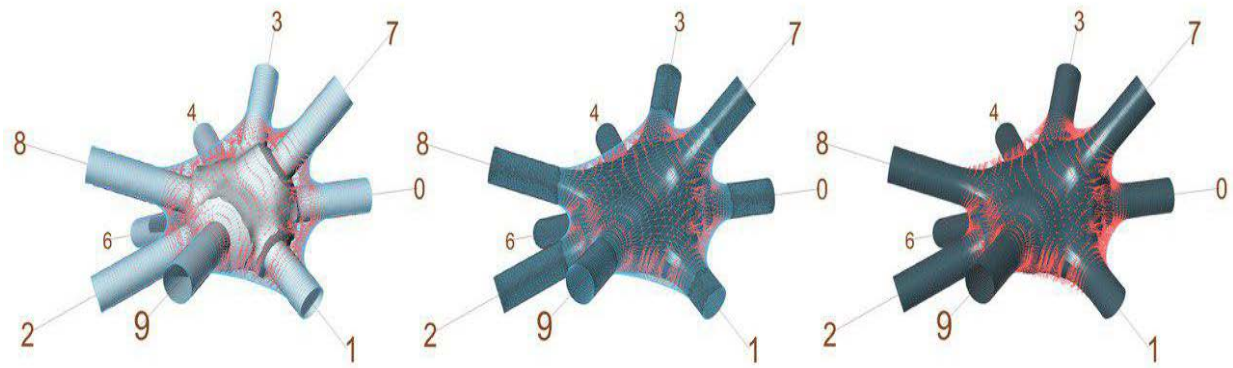


Figure 17. Generating Displacement Vectors and Translating EXO-Mesh

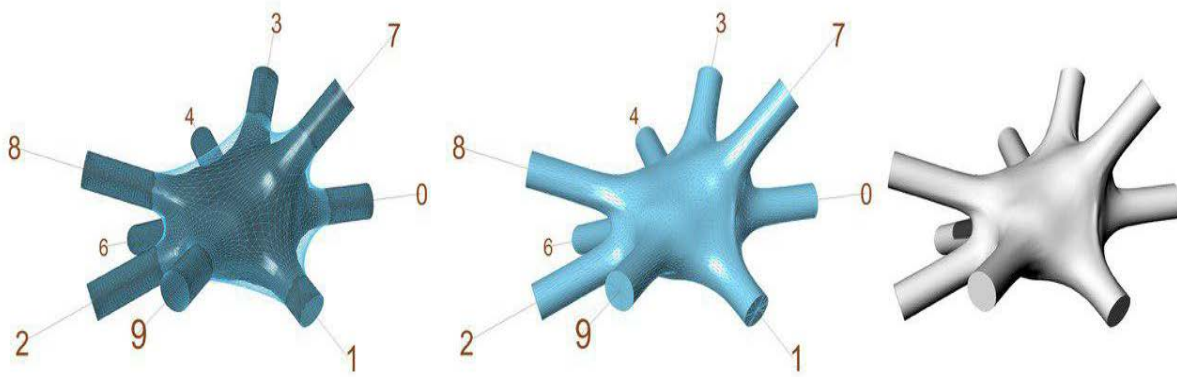


Figure 18. Refinement and Smoothing of the EXO-Mesh, Transformation into a Solid Mesh

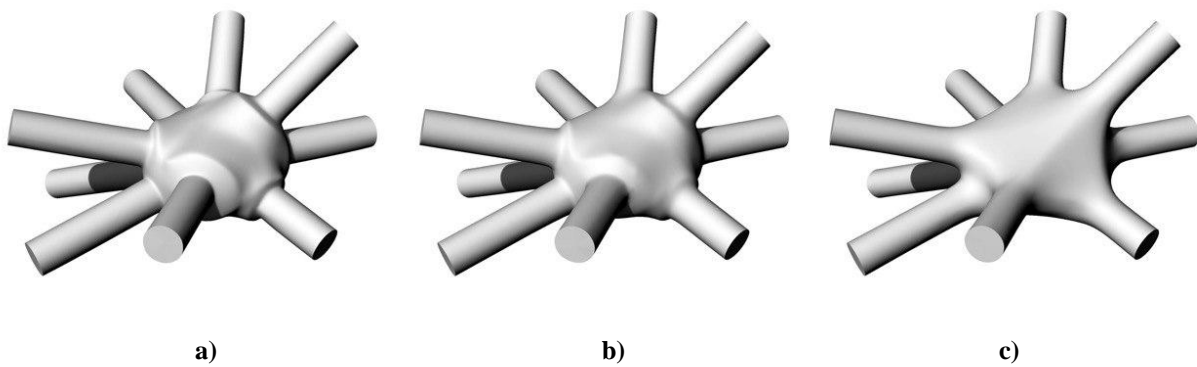


Figure 19. Output Node with Different Percentage of Rationalization a) $a = 20\%$, b) $a = 40\%$ and c) $a = 90\%$

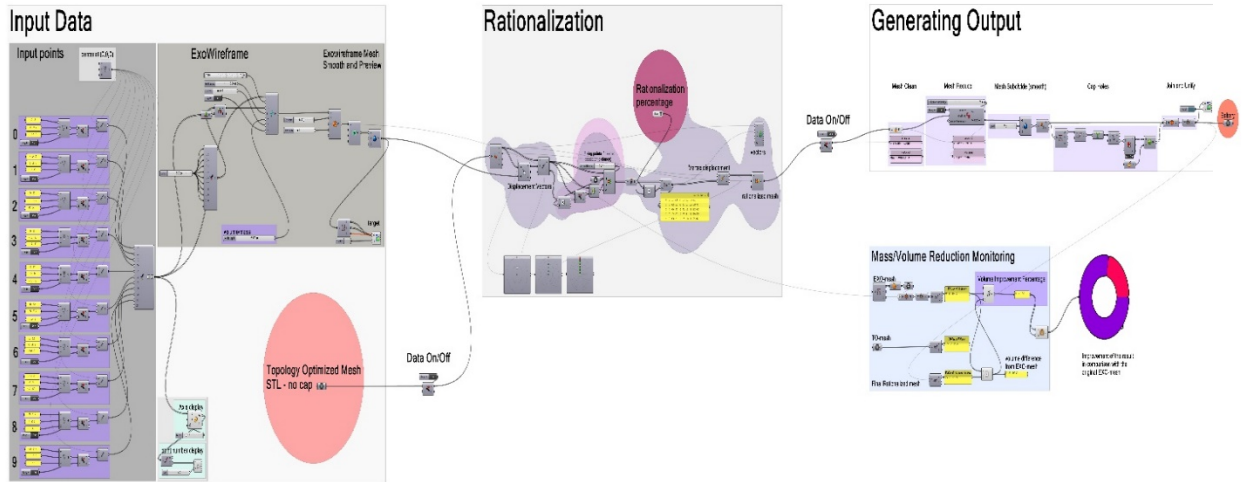


Figure 20. Overview of the Rationalization Process

In order to accomplish all these tasks, we set up an algorithm in Grasshopper with three main sections: a) feeding/creating input data, b) running rationalization algorithm, and c) generating the solid mesh output (Figure 20). The first section focuses on providing the parameters to initialize the node as a network of connected lines, centered at (0,0,0). This information is arisen from the original design of the SF structure, specific for each node. The TO-mesh from solidworks is superimposed to the respective EXO-mesh (Figure 21).

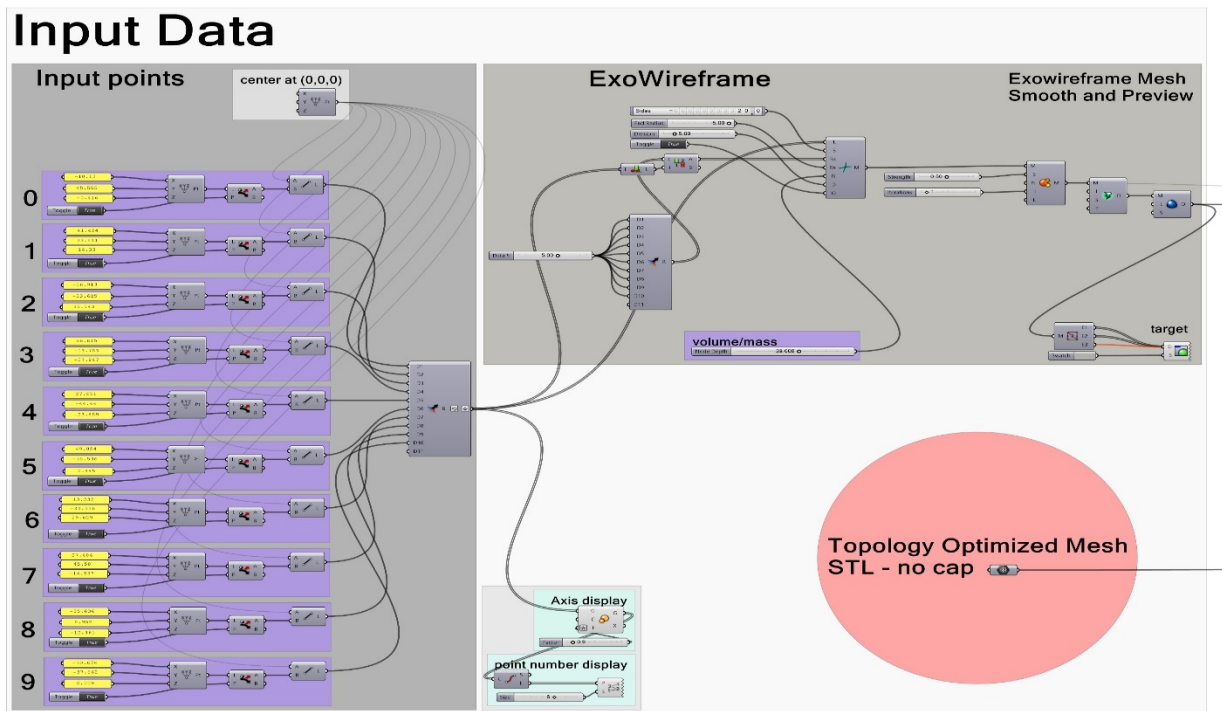


Figure 21. First Part of the Rationalization Algorithm: Setting the Input Data for Exo-Mesh and Imported STL File of TO-Mesh

The second stage is the rationalization module, where all the vectors from TO-mesh towards EXO-mesh are generated and the values for displacement are enumerated (Figure 22). In this stage, the percentage of rationalization is changed and the results are previewed (examples illustrated in Figure 19). At the end of this stage, a new mesh with displaced vertices is created which needs final improvement before exporting the output.

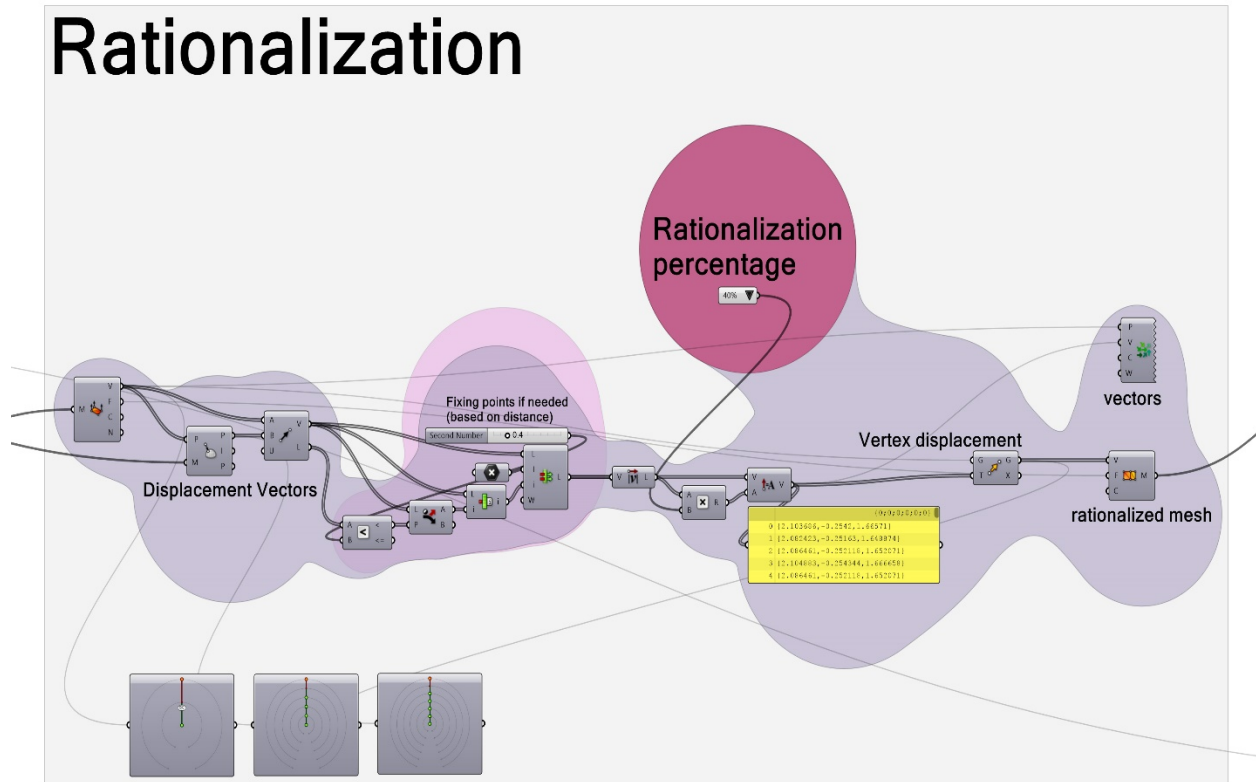


Figure 22. Rationalization Block

During the process of displacing mesh vertices, there are incidents that the mesh might face some interconnections, face/vertex overlap, or in some cases, manifolds, resulting in a “bad” mesh situation. To tackle such issues, there are multiple mesh cleaning strategies/tools that could be used to remove such problematic areas from the output. One of the other challenges in the process is to carry forward unnecessary details from the TO-mesh which is not suitable for fabrication. Excessive details represent too many vertices. In fact, there should be a correlation between the size of the node, its geometrical complexity and the number of vertices, which comprises its mesh. This issue can be addressed by reducing the number of vertices up to the threshold that maintains its quality (this could be done either visually or by setting an average value for the number of vertices per unit area that best represents the required quality). Figure 23 previews the final stage of cleaning/refining the resultant mesh, reducing the size, smooth the surface and finally cover discontinuities (holes) and prepare it for further finite element analysis and fabrication processes. Eventually, the output of the process is a fine solid mesh, which could be used for 3D printing (the implementation of struts, screws, bolts or any geometrical modifications needed for the assembly of the project are not addressed).

Generating Output

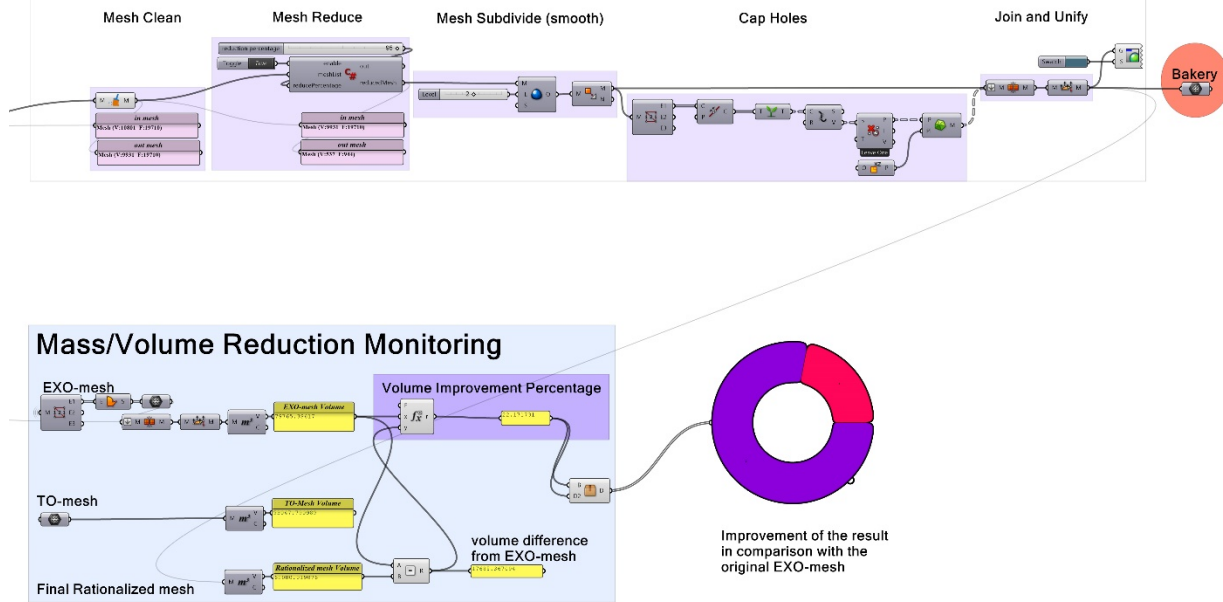


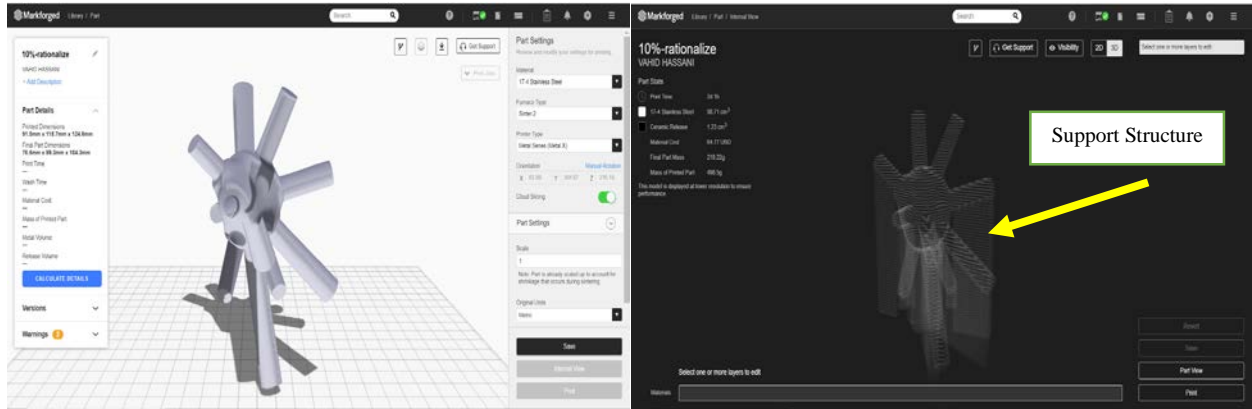
Figure 23. Mesh Refinement Block

4. Method Investigation

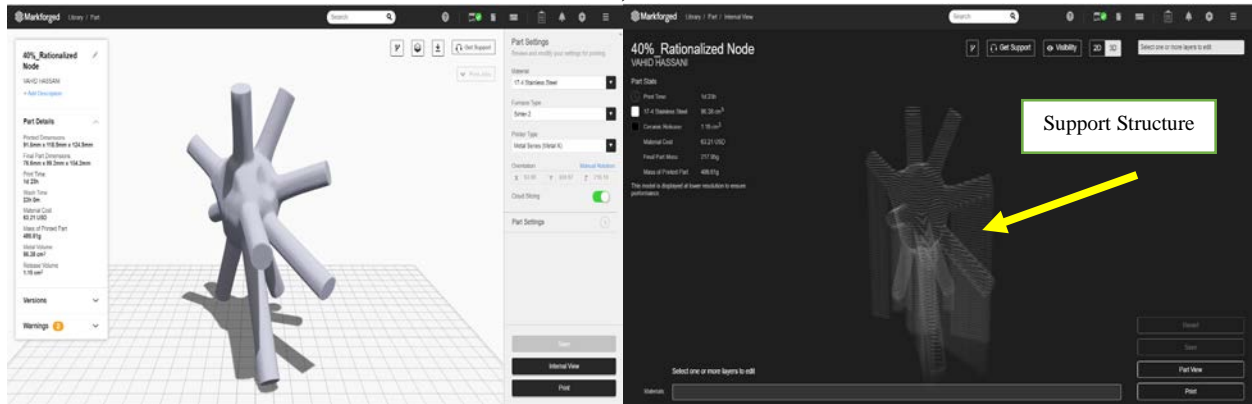
The nodes designed by the topology optimization and rationalized by the mesh-matching technique discussed in previous section, were investigated by Markforged metal printer software in terms of the generated support structure. The printer that works based on Fusion Deposition Melting (FDM) contains filament of 17-4 PH stainless steel. This material that creates metal parts with good mechanical properties, can be produced in both heat treated and non-heat treated condition. The part printed by this material can be easily machined, welded and polished, and offers excellent wear resistance. Using FDM metal printing technology, industries are able to produce parts directly from CAD models by precisely controlling the deposition of filaments onto a build platform. This 3D printing process offers increased design flexibility, reduced manufacturing cost and shortened lead times.

The support structure generation at different degrees of rationalization i.e. 10%, 40% and also 90% are shown in figures 24, 25 and 26 at three different orientations on the build platform, one with random orientation shown in Figure 24, one with minimum printing time orientation shown in Figure 25 and one with minimum generated support structure shown in Figure 26. As seen in Figure 27, higher rationalization degrees will offer more smoothed parts, which are easily printable in real application, however they are accompanied with slightly increase in weight. In terms of the support structure, one can observe the amount of the support structure is decreasing by increasing the rationalization degree at three different orientations. E.g., at the first random orientation, this value is decreasing from 280gr to 259gr respectively from 10% rationalization to 90% and at the second orientation, this value is decreasing from 327gr to 317gr respectively from 10%

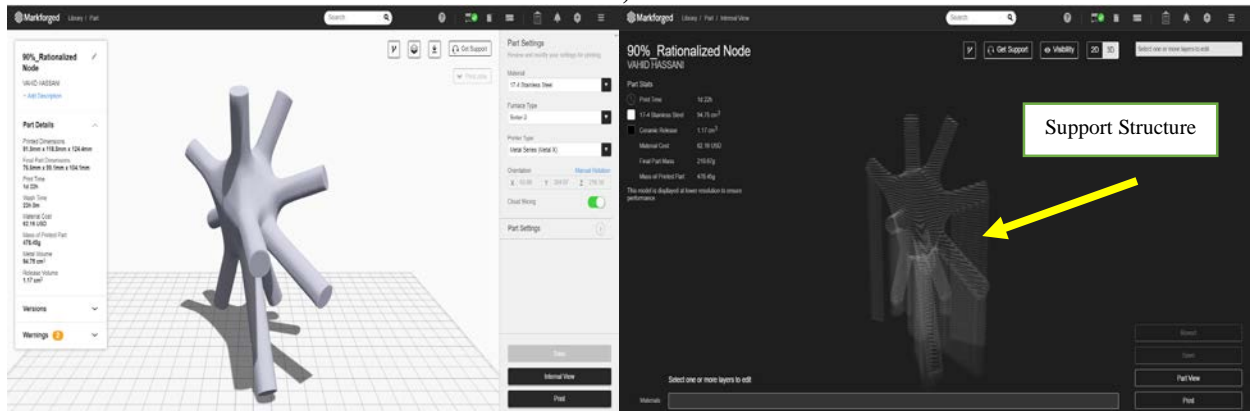
rationalization to 90% and finally at the third orientation, this value is decreasing from 260gr to 247gr respectively from 10% rationalization to 90%.



First Random Orientation - 10% Rationalized Node **Calculated Support Structure by Software: 280gr**
a)

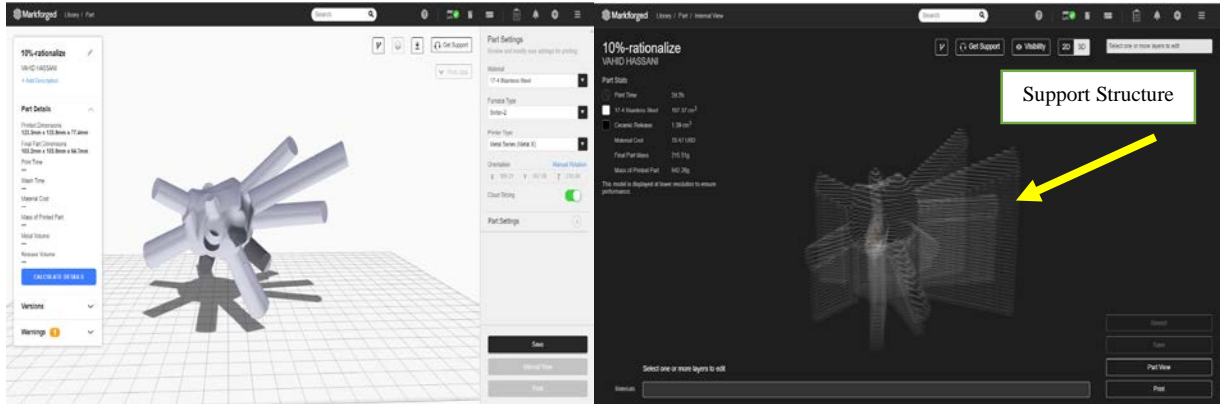


First Random Orientation - 40% Rationalized Node **Calculated Support Structure by Software: 269gr**
b)



First Random Orientation - 90% Rationalized Node **Calculated Support Structure by Software: 259gr**
c)

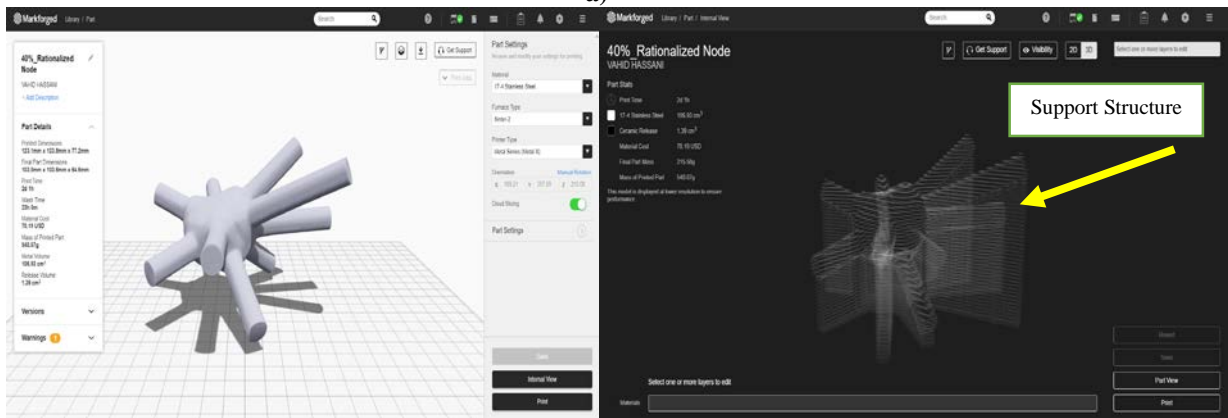
Figure 24. First Random Orientation on the Build Platform, a) 10% Rationalized Node, b) 40% Rationalized Node and c) 90% Rationalized Node



Second Orientation - 10% Rationalized Node

Calculated Support Structure by Software: 327gr

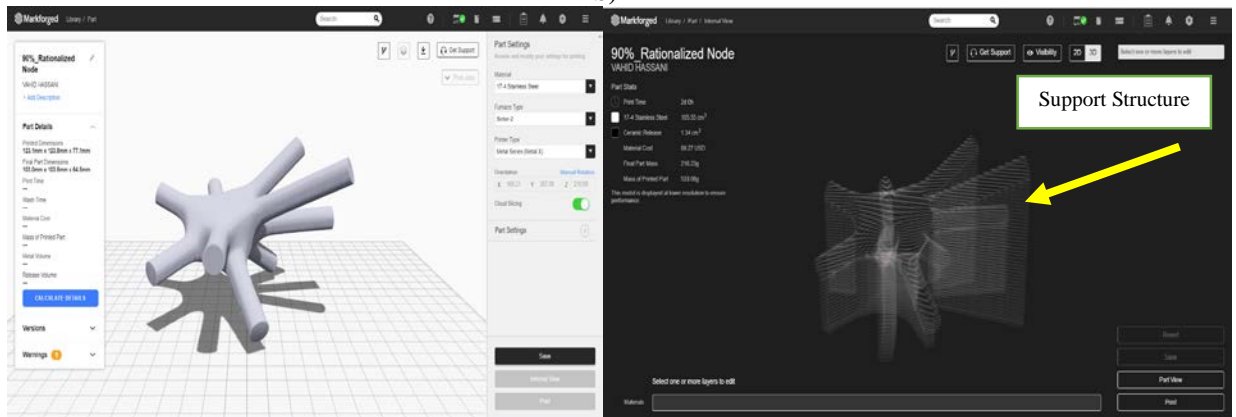
a)



Second Orientation - 40% Rationalized Node

Calculated Support Structure by Software: 325gr

b)

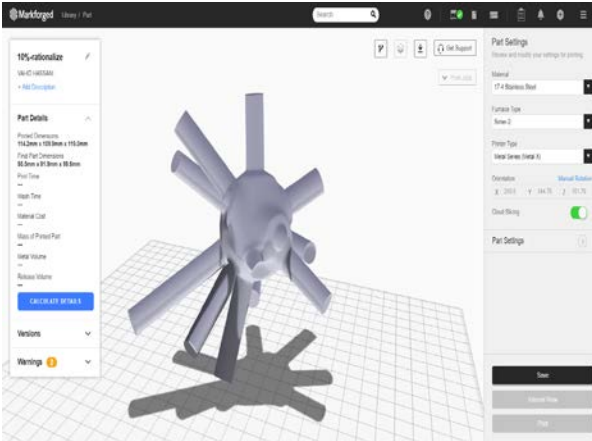


Second Orientation - 90% Rationalized Node

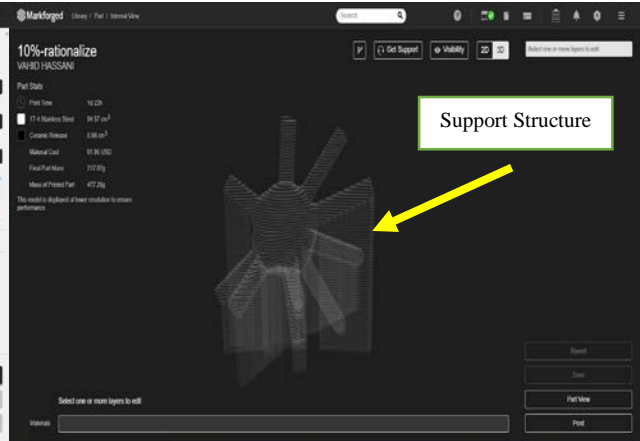
Calculated Support Structure by Software: 259gr

c)

Figure 25. Second Orientation on the Build Platform, a) 10% Rationalized Node, b) 40% Rationalized Node and c) 90% Rationalized Node

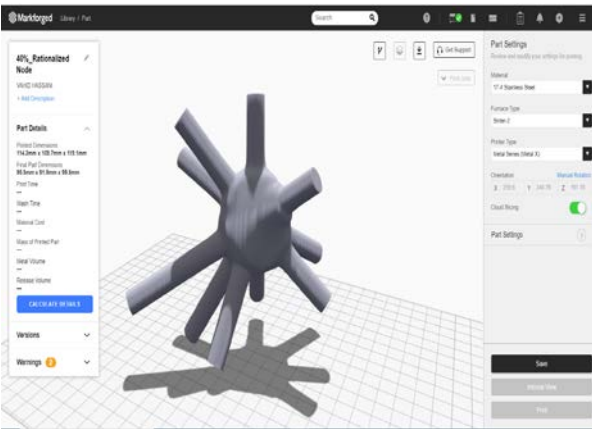


Third Orientation - 10% Rationalized Node

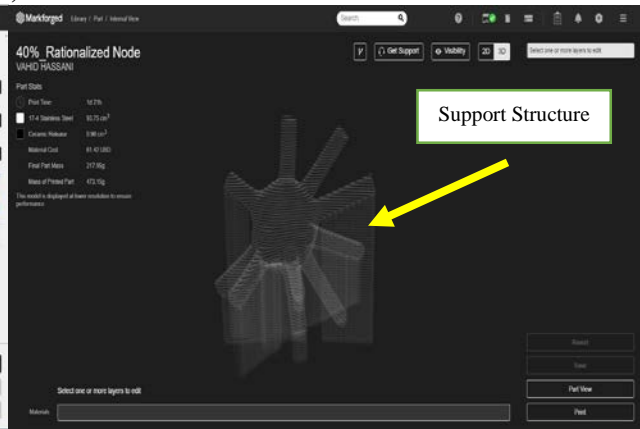


Calculated Support Structure by Software: 260gr

a)

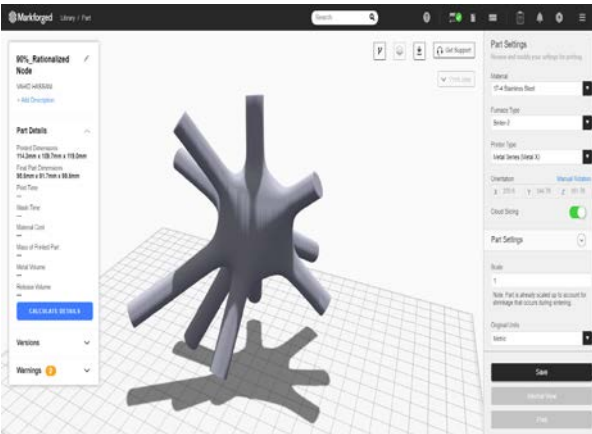


Third Orientation - 40% Rationalized Node

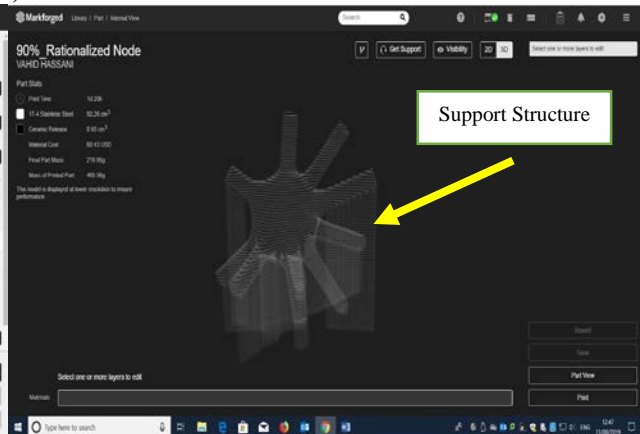


Calculated Support Structure by Software: 256gr

b)



Third Orientation - 90% Rationalized Node



Calculated Support Structure by Software: 247gr

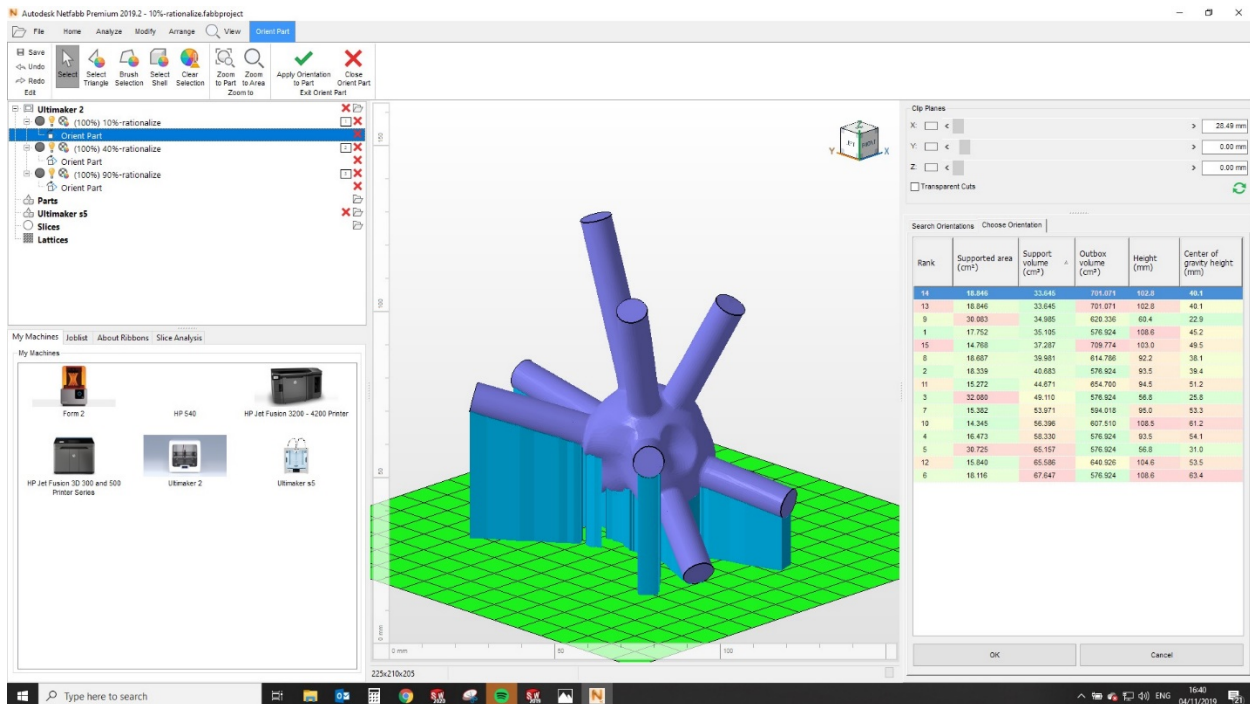
c)

Figure 26. Third Orientation on the Build Platform, a) 10% Rationalized Node, b) 40% Rationalized Node and c) 90% Rationalized Node



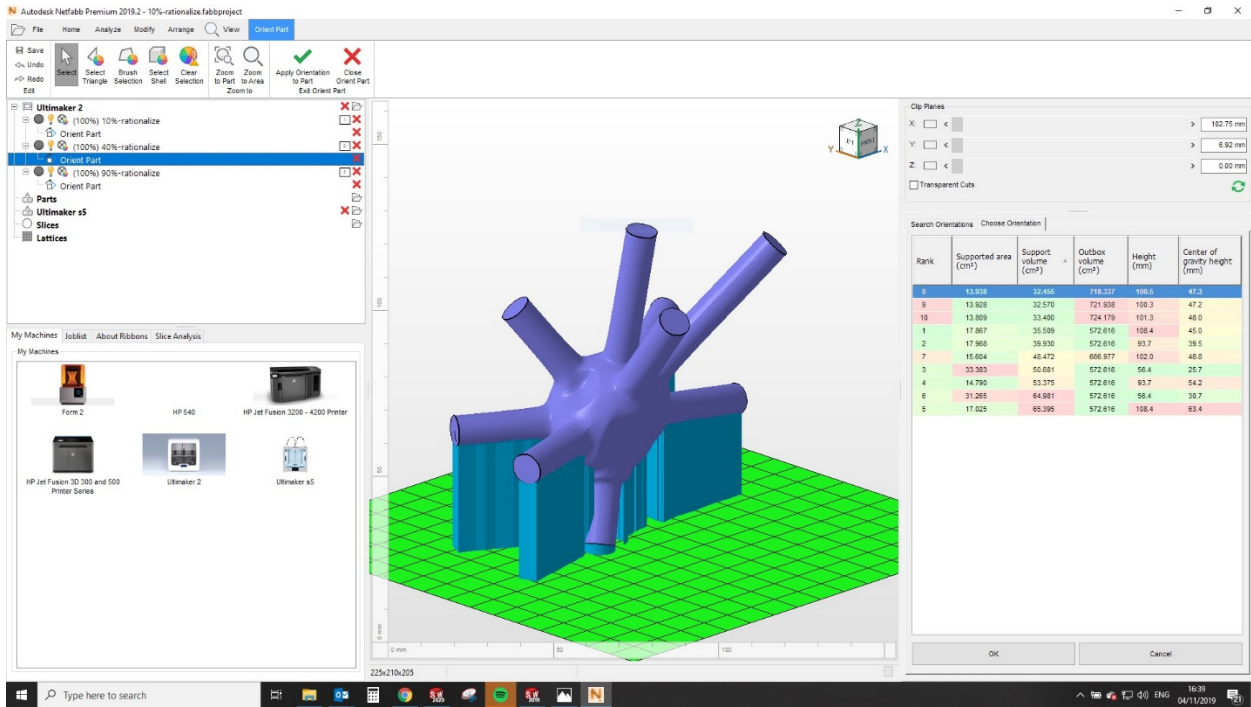
Figure 27. Metal Printed 90% Rationalized Node

In addition to performing the mass calculation of the support structure at three orientations by Markforged metal printer software, namely Eiger, further analysis in Autodesk Netfabb confirms that the volume of the generated support structure will decrease by increasing the rationalization degree. These orientations can also be exported to the Markforged metal printer software. As seen in Figure 28, at the optimum orientation of each node in terms of the minimum support structure, the values of 33.645 cm^3 , 32.455 cm^3 and 30.517 cm^3 have been obtained for 10%, 40% and 90% rationalized nodes, respectively.

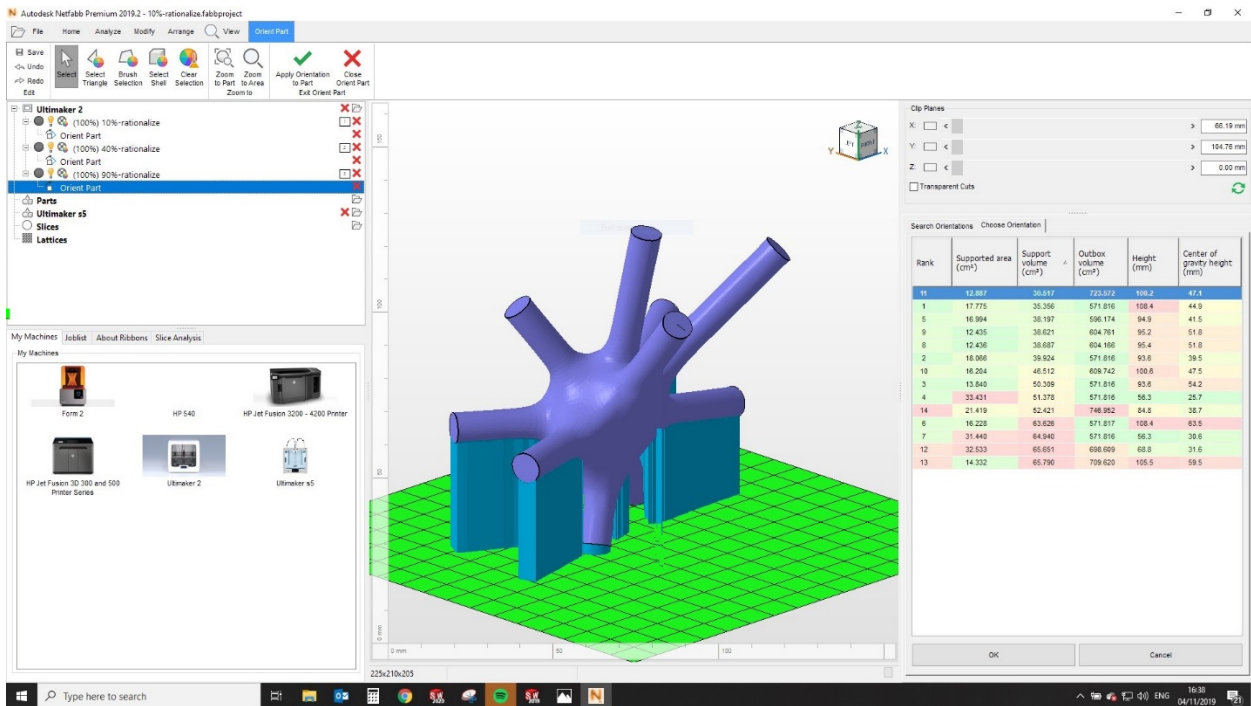


a) 10% Rationalized Node

Figure 28. Continued



b) 40% Rationalized Node



c) 90% Rationalized Node

Figure 28. Optimum Orientation of the Nodes based on Minimum Volumetric Support Structure Calculated at Netfabb Software, a) 10% Rationalized Node, b) 40% Rationalized Node and c) 90% Rationalized Node

In addition to investigation of the nodes in terms of the generated support structure, two static analysis, one under branch forces as shown earlier in Figure 10 and the other under body force of 1000 N, were performed on original topologically-optimized node, 20% rationalized node, 40% rationalized node and also 90% rationalized node in order to compare the different static responses and other properties of interest. When the body force of 1000 N is applied on the volume of each node along z-direction (vertically), the boundary condition is assumed fixed along local coordinates i.e., t1, t2 and n directions at the face of each branch as shown in Figure 11.

Figure 29 shows the results of von Mises stress analysis for the nodes under branch forces and Figure 30 shows the results when the body force of 1000 N applied to the node. As illustrated, maximum von Mises stress is decreasing as the degree of rationalization is increasing.

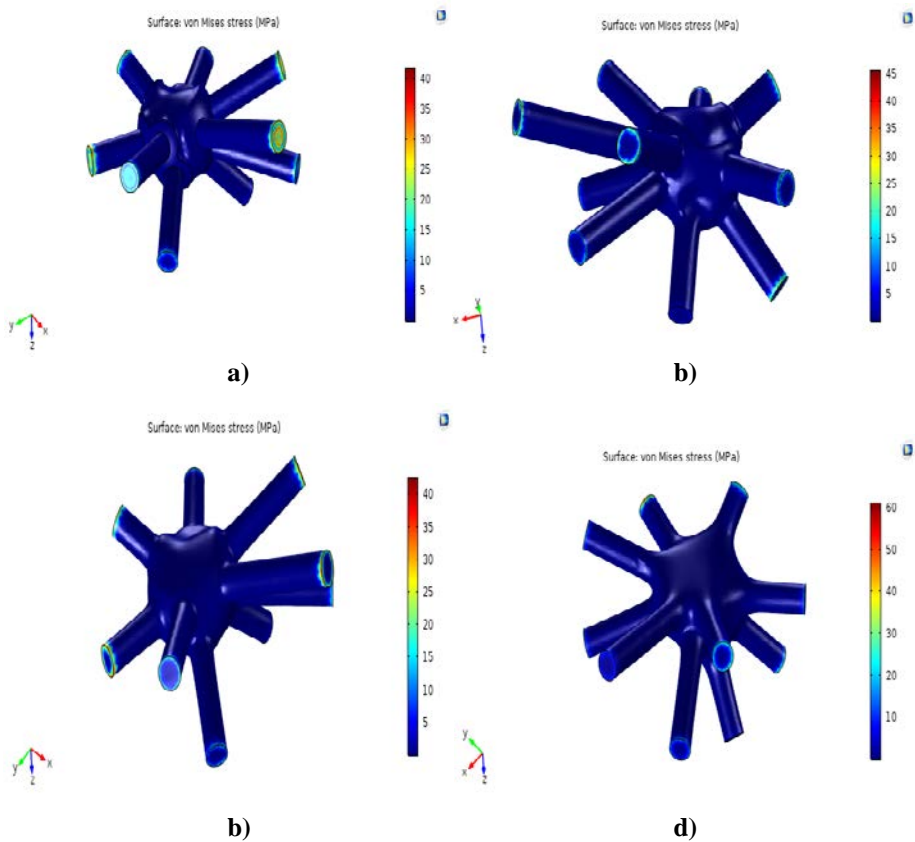


Figure 29. Results of Static Analysis under Branch Force for each Node, a) Original Node: 50 MPa, b) 20% Rationalized: 47 MPa, c) 40% Rationalized: 45 MPa, d) 90% Rationalized: 40 MPa

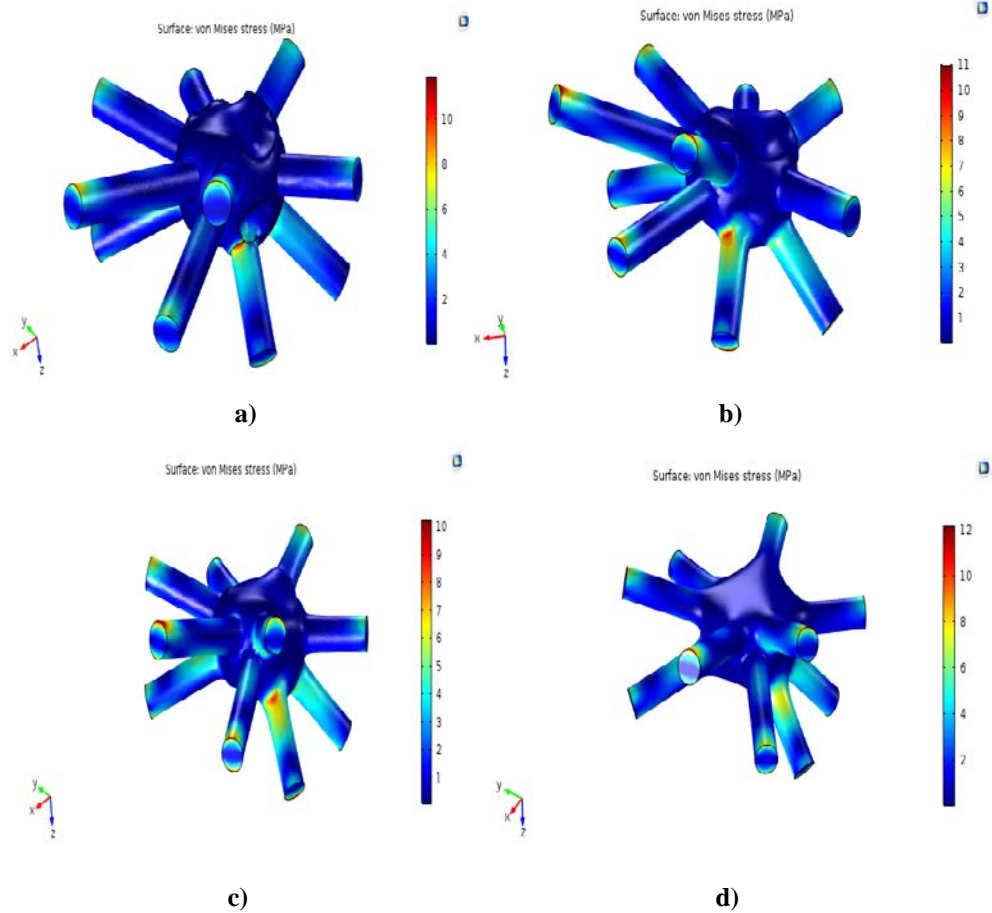


Figure 30. Results of Static Analysis under Body Force of 1000 N for each Node, a) Original Node: 12 MPa, b) 20% Rationalized: 11 MPa, c) 40% Rationalized: 10 MPa, d) 90% Rationalized: 9 MPa

The structural characteristics of the nodes are compared before and after rationalization process in tables 2 and 3. The decrease of 20% of maximum von Mises stress for the branch force scenario and 25% for the body force scenario are observed. The values of strain energy per unit volume reveals 24% decrease for the branch force scenario and 21% decrease for the body force scenario after rationalization. One important point that should be noted is the variation of mass before and after rationalization process. As seen, the original topologically-optimized node has 0.4 kg mass that only increases up to 0.42 kg after 90% rationalization. This proves that the mass is not increasing with the same percentage of rationalization in this method and this characteristic can be considered as one of the strongest point of this method. The increase of 5% mass is advantageous compared to the improvement of 20%-25% for maximum von Mises stress. The mass values for each node is also shown in tables 2 and 3.

Table 2. Comparison of Structural Characteristics before and after Rationalization under Branch Force Analysis

Mechanical Characteristics	Original Topologically-Optimized Node	20% Rationalized Node	40% Rationalized Node	90% Rationalized Node
von Mises Stress (MPa)	50	47	45	40
Mass (kg)	0.4	0.405	0.41	0.42
Strain Energy per Unit Volume (J/m³)	10875	9784	9000	8260

Table 3. Comparison of Structural Characteristics before and after Rationalization under Body Force Analysis

Mechanical Characteristics	Original Topologically-Optimized Node	20% Rationalized Node	40% Rationalized Node	90% Rationalized Node
von Mises Stress (MPa)	12	11	10	9
Mass (kg)	0.4	0.405	0.41	0.42
Strain Energy per Unit Volume (J/m³)	712	682	638	560

5. Conclusions

In this study, an initial configuration of the SF's node was proposed in terms of a multi-branch spherical node as a working platform. The central solid spherical part was topologically-optimized in order to take advantage of obtaining higher stiffness given the initial non-optimized mass distribution. The design procedure was pursued by proposing a rationalization algorithm to clean the sharp edges and indents of the original topologically-optimized node with different degrees and intensities. The nodes with different degrees of rationalization were investigated using Markforged metal printer software and Autodesk Netfabb in terms of the generated support structure that has direct effect on the post-processing time, price and quality of the part. Finally, an static analysis on the original and rationalized nodes demonstrated that the rationalization algorithm introduced in this study, will deliver higher structural properties versus the insignificant expense of added weight. Furthermore, it was explored that the rationalized nodes will offer higher safety and more smooth structure compared to the original topologically-optimized node.

References

- [1]. B. Kolarevic, *Architecture in the Digital Age: Design and Manufacturing*, Taylor and Francis Group, New York and London, (2003).
- [2]. B. Kolarevic, K. Klinger, *Manufacturing Material Effects, Rethinking Design and Making in Architecture*, Routledge, New York, (2008).
- [3]. S. Dritsas, *Design-Built Rationalization Strategies and Applications*, *International Journal of Architectural Computing*, 10 (2012) 575-593.
- [4]. G. Austern, I. G. Capeluto, Y. J. Grobman, *Rationalization Methods in Computer Aided Fabrication: A Critical Review*, *Journal of Automation in Construction*, 90 (2018) 281-293.
- [5]. A. Schlueter, T. Bonwetsch, *Design Rationalization of Irregular Cellular Structures*, *International Journal of Architectural Computing*, 06 (2008) 197-211.
- [6]. T. Fischer, *Geometry Rationalization for Non-Standard Architecture*, *Journal of Architecture Science*, 5 (2012) 25-47.
- [7]. A. B. Larena, D. Azagra, *Searching for the Right Form – The Role of Structural Engineers in the Design of Two Complex-Geometry Buildings in Madrid*, *The Structural Engineer*, 88 (2010) 28-34.
- [8]. T. Fischer, *Geometry Rationalization for Non-Standard Architecture*, *Journal of Architecture Science*, 5 (2012) 25-46.
- [9]. R. Mensil, C. Douthe, O. Baverel, B. Leger, *Generalized Cyclidic Nets for Shape Modeling in Architecture*, *International Journal of Architectural Computing*, 15 (2017) 148-168.
- [10]. S. Darvishani-Fikouhi, *Honeycomb Topologies; Design Rationalization of A Free-Form Space Frame Structure*, Master of Science Thesis, University College London, September (2009).
- [11]. K. Zaremba, *Application of The Genetic Algorithm for A Geometry Rationalization of A Load-Bearing Structure for Free-Form Roof*, *Journal of Procedia Engineering*, 161 (2016) 1722-1730.
- [12]. C. K. Lim, *A Framework for CAD/CAM Design and Construction Process in Freeform Architecture: A Case Study*, *International Journal of Architectural Computing*, 08 (2010) 301-317.
- [13]. G. Austern, I. G. Capeluto, Y. J. Grobman, *Evaluating the Buildability of Architectural Geometries: Embedding Fabrication Awareness into the Design of Concrete Elements*, 6th Annual International Conference on Architecture and Civil Engineering, Singapore, (2018).
- [14]. M. Stavric, M. Manahl, A. Wiltsche, *Discretization of Double Curved Surface, Challenging Glass 4 & COST Action TU0905 Final Conference-Louter, Bos & Belis (Eds)*, (2014) 133-140.
- [15]. N. Baldassini, H. Pottmann, J. Raynaud, A. Schiftner, *New Strategies and Developments in Transparent Free-Form Design: From Facetted to Nearly Smooth Envelopes*, *International Journal of Space Structures*, 25 (2010) 185-197.
- [16]. M. Manahl, M. Stavric, A. Wiltsche, *Ornamental Discretization of Free-Form Surfaces: Developing Digital Tools to Integrate Design Rationalization with the Form Finding Process*, *International Journal of Architectural Computing*, 10 (2012) 595-612.

- [17]. P. Szalabaj, The Digital Design Process in Contemporary Architectural Practice, Session 15: Digital Design Methods – eCAADe 23, (2014) 751-759.
- [18]. S.Galjaard, S.Hofman, S.Ren, New Opportunities to Optimize Structural Designs in Metal by Using Additive Manufacturing, In: Advances in Architectural Geometry, (2014) 79-93.
- [19]. C.T.Mueller, 3D Printed Structures: Challenges and Opportunities, Structure, 54 (2016).
- [20]. S. Ren, S. Galjaard, Topology Optimization for Steel Structural Design with Additive Manufacturing, Journal of Modeling Behavior, (2015) 35-44.
- [21]. M.Seabra, J.Azevedo, A.Araujo, L.Reis, E.Pinto, Selective Laser Melting (SLM) and Topology Optimization for Lighter Aerospace Components, Procedia Structural Integrity, 1 (2016) 289-296.
- [22]. Wohler's Report: 3D Printing and Additive Manufacturing State of the Industry, Annual Worldwide Progress Reprt, (2018).
- [23]. M.P.Bendsoe, O.Sigmund, Topology Optimization: Theory, Methods and Applications, Second Edition, Springer, (2003).
- [24]. Y. Zhou, T. Nomura, K. Saitou, Multi-Component Topology Optimization for Powder Bed Additive Manufacturing (MTO-A), Proceedings of the ASME 2018 International Design Engineering, Technical Conferences and Computers and Information in Engineering Conference, IDETC/CIE 2018, August 26-29, 2018, Quebec City, Quebec, Canada, (2018).
- [25]. T. Wu, A. Tovar, Design for Additive Manufacturing of Conformal Cooling Channels using Thermal-Fluid Topology Optimization and Application in Injection Molds, Proceedings of the ASME 2018 International Design Engineering, Technical Conferences and Computers and Information in Engineering Conference, IDETC/CIE 2018, August 26-29, 2018, Quebec City, Quebec, Canada, (2018).
- [26]. K. Wachsmann, The Turning Point of Building: Structure and Design, Reinhold Publication Corporation, (1961).
- [27]. D. Stasiuk, Exoskeleton, <https://www.grasshopper3d.com/group/exoskeleton>, (2014).
- [28]. V. Hassani, Z. Khabazi, F. Raspall, C. Banon, D.W. Rosen, Form-Finding and Structural Shape Optimization of the Metal 3D-Printed Multi-Branch Node with Complex Geometry, Computer-Aided Design and Applications (CADA), 17 (2019) 205-225.
- [29]. C.Preisinger, Linking Structure and Parametric Geometry, Architect Design, doi:10.1002/ad.1564, 83 (2013) 110-113.